BMC Genomics

RESEARCH Open Access

Exploring the toxicological mechanisms of reduced fertility in dairy cows due to nonesterified fatty acids on the basis of network toxicology, transcriptomics and molecular docking

Junkai Wang[1,2], Wenjing Wang[1], Xiaoqi Kang[1], Yaqian Liang[1], Lulu Li[2*], Yuqing Liu[2*] and Haihong Hao[1,3*]

Abstract

High concentrations of nonesterified fatty acids (NEFAs) are normal metabolites of high-producing dairy cows in a state of negative energy balance (NEB), but they are thought to be strongly associated with reproductive disorders in dairy cows, which may contribute to reduced fertility in cows (RFC). There are few studies on the independent toxic effects of NEFA-mediated RFC. This study aimed to investigate the toxicological effects of NEFA-mediated RFC systematically via network toxicology, transcriptomics, and molecular docking techniques. A total of 403 potential targets of NEFA-mediated RFC toxicity were screened by comprehensively analyzing the *GeneCards*, *OMIM*, *ChEMBL* and *Swiss Target Prediction* databases. Further analysis via the *GEO* (GSE165476 dataset), *STRING* databases and *Cytoscape* software yielded eight hub targets, including MMP2, MAPK1, PRKACA and PRKCB. Gene Ontology (GO) and Kyoto Encyclopedia of Genes and Genomes (KEGG) pathway enrichment analyses revealed that these targets were involved in pathways related to metabolism, endocrine processes, cell death, and signal transduction, such as the AGE-RAGE signaling pathway in diabetic complications, the GnRH signaling pathway, and the MAPK signaling pathway. Molecular docking further confirmed the potential interactions between NEFAs and these hub targets. This study revealed that NEFAs may exacerbate the occurrence of RFC by interfering with endocrine regulation, inducing inflammatory responses, affecting angiogenesis and tissue remodeling, regulating apoptosis, and disrupting metabolic balance. The results of this study provide novel molecular insights into the mechanism of NEFA-mediated RFC toxicity and provide a scientific basis for emphasizing the importance of metabolite toxicity in dairy farming health management.

Keywords Network toxicology, NEFAs, Reduced fertility in cows, Transcriptomics, Molecular docking

*Correspondence:
Lulu Li
luluscau@126.com
Yuqing Liu
liuiuqing@163.com
Haihong Hao
haihong_hao@aliyun.com

[1]Key Laboratory of Control and Prevention of Animal Disease, College of Animal Science and Technology, Shihezi University, Shihezi, China
[2]Shandong Key Laboratory of Animal Disease Control and Breeding, Institute of Animal Science and Veterinary Medicine, Shandong Academy of Agricultural Sciences, Jinan, China
[3]National Reference Laboratory of Veterinary Drug Residues, Huazhong Agricultural University, Wuhan, China

Introduction

A decrease in reproductive performance is the main reason for the premature culling of dairy cows worldwide, leading to reduced milk yield, fewer calves, and substantial economic losses. Losses of 70–220 dollars per cow per year have been reported in the United States when the calving-to-conception interval is 130–160 days [1]. Transitional cows reduce their dry matter intake (DMI) prior to calving, require more energy for milk production than they consume, and generally enter a state of NEB—a condition often exacerbated by deficiencies in vitamins A and E [2]. In response to these conditions, cows mobilize substantial amounts of lipids, which are broken down to generate large quantities of NEFAs; these then diffuse into the bloodstream to supply energy for the entire body. However, high levels of NEFAs can cause anorexia in cows, which may exacerbate NEB deterioration and promote lipid metabolism and NEFA loading [3, 4].

NEFA is a collective term for a class of compounds, among which the most abundant fatty acids are oleic acid (OA; C18:1), palmitic acid (PA; C16:0) and stearic acid (SA; C18:0) [5]. Currently, numerous studies have shown that excess NEFAs are strongly associated with reproductive disorders and thus may lead to RFC. Ribeiro et al. demonstrated that NEFA concentrations in the first 10 days post-partum in dairy cows are strongly negatively correlated with the development of uterine diseases [6]. Kaneene et al. reported that elevated NEFA concentrations increase the risk of metritis and placenta retention [7]. Macmillan et al. demonstrated that higher serum NEFA concentrations in early postpartum cows were associated with lower fertility [8]. Therefore, high concentrations of NEFAs are not only energy-related indicators of massive lipid mobilization but also potential metabolic toxicants.

Despite growing evidence linking NEFAs to reproductive dysfunction, most studies have focused on isolated outcomes rather than exploring the broader molecular mechanisms. Previous studies have focused mostly on the impact of NEFAs on single indicators such as the conception rate in dairy cows [6, 9, 10]. Although some studies have demonstrated the toxic effects of high concentrations of NEFAs on oocytes [11, 12], the specific and systematic molecular mechanisms of toxicity are not clear. In addition, NEB status in cows is accompanied by multiple hormonal and metabolic changes, making it difficult to accurately isolate the independent toxic effects of NEFAs and their interaction networks in this complex context.

Network toxicology integrates the principles of network pharmacology and systems biology and involves constructing a network of compounds, toxins and targets with the help of bioinformatics, big data analysis and multiomics technology to reveal complex biological mechanisms [13]. Transcriptomics can directly reveal differential expression profiles at the genome-wide level in tissues exposed to compounds, thereby identifying key differentially expressed genes (DEGs) and functional modules. Molecular docking computationally simulates the binding capacity of targets and compounds, validating their direct interaction and providing molecular-level evidence to support predictive results from network toxicology and transcriptomics [14]. Together, these approaches offer a comprehensive and efficient strategy to elucidate the molecular mechanisms underlying NEFA-induced reproductive toxicity.

This study aims to systematically investigate the potential molecular toxicity mechanisms of NEFA-mediated RFC through network toxicology, transcriptomics, and molecular docking to provide new toxicological insights for understanding the effects of NEFAs on RFC. The detailed experimental procedure is shown in Fig. 1.

Materials and methods

Prediction of NEFA toxicity

We retrieved the molecular information and simplified molecular input line entry system (SMILES) representations of high-NEFA (PA, SA, and OA) from the *PubChem* database (https://pubchem.ncbi.nlm.nih.gov). Toxicity predictions for these NEFAs were subsequently conducted using their SMILES representations as inputs via the *ProTox3* (https://tox.charite.de) and *ADMETlab 3.0* (https://admetlab3.scbdd.com) platforms. Given the critical role of peroxisome proliferator-activated receptor γ (PPARγ) in both lipid metabolism and reproductive regulation [15], the evaluation criterion was established as follows: a compound was deemed toxic if PPARγ activation was predicted by at least one platform.

Identification of NEFA target genes

We used the ChEMBL (https://www.ebi.ac.uk/chembl/), Swiss Target Prediction (http://www.swisstargetprediction.ch/), OMIM (https://omim.org/), and GeneCards (https://www.genecards.org/) databases to identify potential targets of NEFAs on the basis of their chemical names or SMILES. The thresholds described in the previous study were referenced and slightly modified [16]; targets with a probability score > 0.1 were selected from the Swiss Target Prediction; the top 5% of the targets were selected from the OMIM; and the top 15% of the targets by score were selected from the GeneCards. To improve the accuracy of the targets and species, after integrating the targets obtained from the 4 databases and removing duplicates, we used the *UniProt* database (https://www.uniprot.org/) to calibrate the targets, with the species selected as "*Bos taurus*".

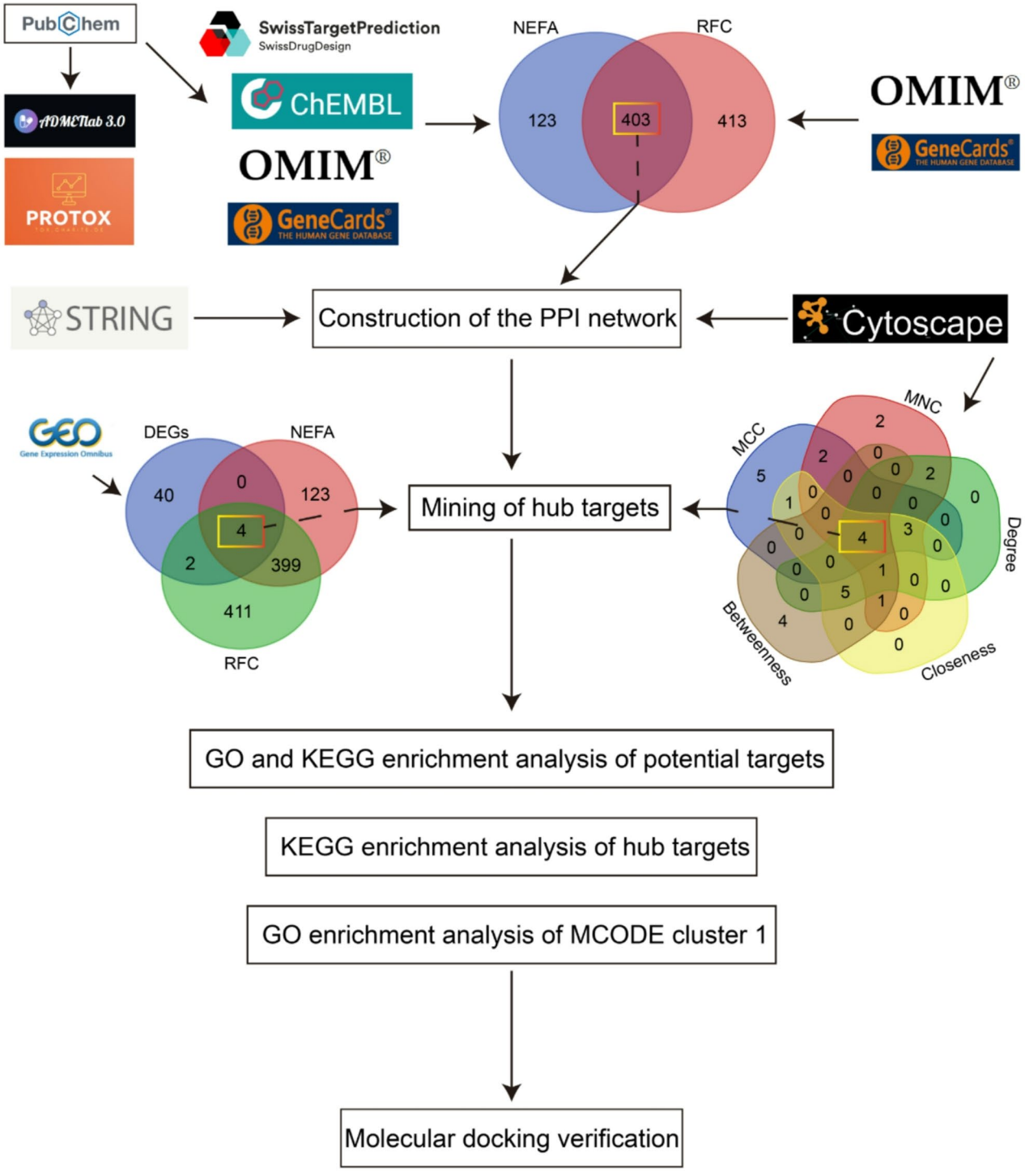

Fig. 1 Overview of study design

Identification of RFC target genes

To include as many RFC-related targets as possible, the keywords "reduced fertility of females" or "reduced reproduction of females" were used to identify potential targets in the GeneCards and OMIM databases. Among these, the top 10% of the targets by score were selected from the GeneCards, and the top 10% of the targets were selected from the OMIM. After the targets obtained from the 2 databases were integrated and duplicates were removed, the targets were curated using the UniProt database, restricted to the species "*Bos taurus*".

Cross-analysis of target sets

The obtained RFC target sets and NEFA target sets were cross-analyzed via the Draw Venn Diagram online tool (https://bioinformatics.psb.ugent.be/webtools/Venn/) to explore overlapping genes, which were designated potential targets for subsequent analyses. The overlapping genes were considered candidate targets for further network and functional analysis. The statistical significance of this overlap was confirmed via a hypergeometric test.

Screening of hub targets and construction of the protein–protein interaction (PPI) network

The aforementioned potential targets were entered into the STRING database (https://cn.stringdb.org/) to con struct a PPI network, with the confidence threshold set to the highest confidence (≥ 0.9) and targets without connections hidden to identify biologically significant PPIs, thereby ensuring the validity of interactions in the network. The PPI network was analyzed and visualized via Cytoscape v3.10.2 software, with nodes representing NEFA or RFC targets and edges representing interactions between the target proteins. The PPI network modules were subsequently clustered via the Molecular Complex Detection (MCODE) plugin to identify gene clusters with similar or identical biological functions; the MCODE score is proportional to their importance in the entire network. The parameters for MCODE analysis were set as follows: degree cutoff = 2, node score cutoff = 0.2, k-core = 2, and maximum depth = 100. The PPI network was ranked according to the MCODE score values, with larger circles and darker nodes representing higher scores. In addition, five algorithms of the CytoHubba plugin—maximum clique centrality (MCC), maximum neighborhood component (MNC), degree, betweenness centrality, and closeness centrality—were used to calculate the overlapping genes among the top 15 genes, and these overlapping genes served as hub genes.

Mining of hub genes via transcriptomics

Determination of the dataset

To further expand the scope of the hub genes, we used the GEO database (https://www.ncbi.nlm.nih.gov/geo/) and selected the dataset GSE165476, which contains bovine ovarian tissues exposed to high concentrations of NEFAs and control samples.

Tissue sample preparation for GSE165476: Ovarian cortical strips were isolated from abattoir-sourced bovine ovaries. The natural follicles were removed, and the remaining cortical strips were randomly assigned to the control tissue culture medium (CON) group or the high-NEFA group (PA, SA and OA).

Quality control and preprocessing of data

To ensure data reliability, we downloaded the raw data of dataset GSE165476 (SRA Study: SRP303183) from the *SRA* database (https://www.ncbi.nlm.nih.gov/sra) and processed the data as follows: Quality control and preprocessing of the raw data were performed via the fastp v0.23.4 tool to remove low-quality sequences and adapter contamination, with the first 12 bp of the reads subsequently trimmed. The processed high-quality reads were aligned to the reference genome (*Bos taurus*.ARS-UCD2.0, release 114) via *STAR* v2.7.10b software to determine gene expression. Next, the expression of each gene in the samples was calculated via the *featureCounts* v2.0.1 tool to generate an expression matrix. On average, 88.11% of the reads were mapped to the genome, with an average of 82.73% uniquely mapped. Finally, principal component analysis (PCA) was performed and visualized via *R* software and the "ggplot2" package.

Screening of DEGs and hub targets

To identify DEGs, differential expression was assessed using empirical Bayes moderation via the "limma" package in R software for statistical analysis. The count data were normalized using the trimmed mean of M-values (TMM) method. The p value was adjusted via the Benjamini–Hochberg method, and the screening criteria were set as $|\log_2 \text{fold change}| \geq 1$ and $p \leq 0.05$. A volcano plot was generated via the "ggplot2" package in R software to visualize the transcriptional differences between the NEFA and control groups. A heatmap of the DEGs was generated via the ChiPlot tool (https://www.chiplot.online/) to visualize the expression profiles of the DEGs. Finally, the DEGs were cross-analyzed with the two aforementioned target sets, and the overlapping genes of the three datasets served as our new hub genes.

GO and KEGG enrichment analyses

GO functional annotation and KEGG pathway enrichment analyses were performed and visualized via the "clusterProfiler", "org.Bt.eg.db", and "ggplot2" packages in R. The screening criterion was set as a false discovery rate (FDR) < 0.05 to explore the potential roles of biological processes, molecular functions, cellular components and signaling pathways associated with the potential targets. In addition, to better explore the key mechanisms of local network modules as well as hub targets in NEFA-induced RFC toxicity, we performed GO term enrichment analysis for MCODE cluster 1, which had the highest modular score, and KEGG enrichment analysis for the hub genes. Finally, to further explore the pathways of NEFA-mediated RFC, we performed cross-analysis of the KEGG analysis results of the potential and aforementioned hub targets.

Table 1 Molecular weight, SMILES structure and PPARγ activation probability of NEFAs

Compound	Molecular weights	SMILES structures	Probability (ADMETlab 3.0)	Probability (ProTox3)
Palmitic acid	256.24 g/mol	CCCCCCCCCCCCCCCC(=O)O	0.852	Inactive
Stearic acid	284.27 g/mol	CCCCCCCCCCCCCCCCCC(=O)O	0.845	Inactive
Oleic acid	282.26 g/mol	CCCCCCCC/C=C\CCCCCCCC(=O)O	0.939	0.9

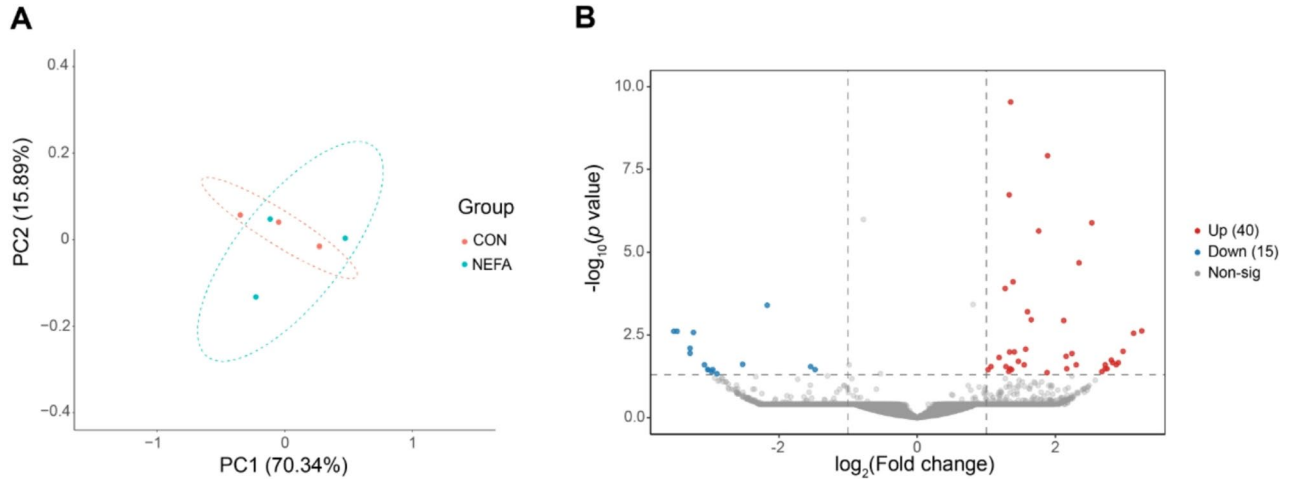

Fig. 2 PCA and DEG analysis of the GSE165476 dataset. **A** PCA of the GSE165476 dataset. CON, control. **B** Volcano plot of the DEGs between the NEFA and control groups (p value ≤ 0.05, $|\log_2$ fold change$|$ ≥ 1)

Molecular docking

To validate the predicted interactions at the molecular level, we performed docking simulations between NEFAs and hub proteins. The PDB files of the hub genes were downloaded from the *AlphaFold Protein Structure* Database (https://alphafold.com/), and the SDF files of high-NEFA (PA, SA, and OA) chemical structures were downloaded from the PubChem database. Molecular docking analysis was performed via the CB-Dock2 platform (https://cadd.labshare.cn/cb-dock2/index.php), and the binding energy was used to assess the molecular docking interactions of the receptors and ligands. A binding energy < − 5.0 kcal/mol is generally considered to indicate stable binding. Finally, a heatmap of binding energy was generated via the ChiPlot tool, and the molecular docking results (binding energy < − 5.0 kcal/mol) were visualized via the CB-Dock2 platform [17].

Results

Assessment of NEFA toxicity

High-concentration NEFAs (PA, SA, and OA) all passed the toxicity prediction assays via the ProTox3 and ADMETlab 3.0 platforms with a high probability (Table 1).

Identification of NEFA-related targets

A total of 1220 targets were obtained by comprehensive analysis of the ChEMBL, Swiss Target Prediction, OMIM and GeneCards databases, and with calibration in the UniProt database, 526 potential NEFA-related targets were ultimately obtained (Supplementary Table 1).

Identification of RFC-related targets

A total of 1933 targets were obtained by integrating the results of the GeneCards and OMIM databases. After calibration via the UniProt database, 816 potential RFC-related targets were ultimately obtained (Supplementary Table 2).

Results of screening the DEGs

PCA was used to assess the overall distribution and variability of gene expression data between the NEFA and control groups. As shown in Fig. 2A, the first principal component (PC1, 70.34%) and PC2 (15.89%) together explained 86.23% of the total variance, indicating a good principal component explanation rate. However, the two samples did not show a clear cluster pattern in the space constituted by these two principal components, indicating that gene expression variability within groups may exceed differences between NEFA and control conditions.

We used a volcano plot to further validate the transcriptional differences between the NEFA and control groups. The volcano plot (Fig. 2B) revealed a total of 55 DEGs, which included 40 upregulated genes (red points; Table 2) and 15 downregulated genes (blue points; Table 3). In addition, a heatmap of the DEGs was generated to visualize the expression levels of these genes in different samples. As shown in Fig. 3, the expression of

Table 2 Transcription results of upregulated DEGs (*p* value ≤ 0.05, $\log_2$(fold change) ≥ 1)

Gene name	Ensembl ID	$\log_2$(fold change)	*p* value
SDF2L1	ENSBTAG00000000067	1.46	$1.98E^{-02}$
ATP10D	ENSBTAG00000000473	2.88	$2.49E^{-02}$
GPNMB	ENSBTAG00000000604	1.89	$1.22E^{-08}$
ADAMTS5	ENSBTAG00000000648	1.59	$6.23E^{-04}$
LGALS3	ENSBTAG00000002326	2.12	$1.15E^{-03}$
ADAMTSL4	ENSBTAG00000003604	2.67	$4.08E^{-02}$
MYO5C	ENSBTAG00000003763	2.24	$1.14E^{-02}$
DPAGT1	ENSBTAG00000005371	2.72	$2.52E^{-02}$
SEMA3C	ENSBTAG00000006138	2.53	$1.30E^{-06}$
SUOX	ENSBTAG00000006160	2.75	$3.31E^{-02}$
MYO5A	ENSBTAG00000006489	1.32	$4.01E^{-02}$
SOD2	ENSBTAG00000006523	1.39	$7.79E^{-05}$
LOC100139670	ENSBTAG00000007881	1.57	$8.48E^{-03}$
SEL1L	ENSBTAG00000008083	1.34	$1.04E^{-02}$
SLC38A2	ENSBTAG00000011105	1.07	$2.85E^{-02}$
CKAP4	ENSBTAG00000011913	1.36	$3.50E^{-02}$
CTSB	ENSBTAG00000012442	1.03	$3.50E^{-02}$
NFE2L1	ENSBTAG00000013653	1.35	$3.31E^{-02}$
SPCS3	ENSBTAG00000014146	1.55	$2.52E^{-02}$
CD9	ENSBTAG00000014764	2.15	$1.39E^{-02}$
TM4SF1	ENSBTAG00000015163	1.28	$2.85E^{-02}$
BTBD2	ENSBTAG00000016108	2.91	$2.17E^{-02}$
FAM180A	ENSBTAG00000017427	3.25	$2.37E^{-03}$
CHI3L1	ENSBTAG00000018223	1.65	$1.09E^{-03}$
ANXA8L1	ENSBTAG00000018499	2.98	$9.83E^{-03}$
S100A4	ENSBTAG00000019203	2.49	$7.85E^{-15}$
MMP2	ENSBTAG00000019267	1.18	$1.52E^{-02}$
FBP2	ENSBTAG00000019554	2.81	$1.81E^{-02}$
DHRS7	ENSBTAG00000020729	2.30	$2.52E^{-02}$
CTSK	ENSBTAG00000021035	1.33	$1.86E^{-07}$
BCAS4	ENSBTAG00000038929	3.13	$2.80E^{-03}$
LOC112444563	ENSBTAG00000043222	1.88	$4.31E^{-02}$
NA	ENSBTAG00000043582	1.76	$2.31E^{-06}$
CFB	ENSBTAG00000046158	2.34	$2.08E^{-05}$
ADAMTSL5	ENSBTAG00000046263	2.83	$2.17E^{-02}$
MT1A	ENSBTAG00000054808	2.16	$3.31E^{-02}$
NA	ENSBTAG00000057732	1.27	$1.23E^{-04}$
NA	ENSBTAG00000057824	2.72	$3.31E^{-02}$
NA	ENSBTAG00000061247	1.35	$2.90E^{-10}$
HERPUD1	ENSBTAG00000076584	1.41	$1.02E^{-02}$

NA Not Applicable

genes within the group was highly consistent, indicating distinct expression profiles between the NEFA group and the control group.

Cross-analysis results of the target sets and DEGs

The NEFA target library, RFC target library and 55 DEGs were cross-analyzed via the Draw Venn Diagram online tool, and a Venn diagram was generated to visualize the results. There were 403 potential target genes overlapping between the NEFA and RFC target sets (Fig. 4A; Supplementary Table 3), 4 of which were DEGs (Fig. 4B). These DEGs were MMP2, CTSB, CTSK, and SOD2, which were all upregulated in the high-concentration NEFA group (Table 2). These overlapping genes were then used to construct a PPI network to identify hub targets.

Table 3 Transcription results of downregulated DEGs (*p* value ≤ 0.05, $\log_2$(fold change) ≤ − 1)

Gene name	Ensembl ID	$\log_2$(fold change)	*p* value
TTI2	ENSBTAG00000015463	−3.03	$4.98E^{-05}$
SORBS2	ENSBTAG00000016486	−2.53	$2.36E^{-05}$
GRB14	ENSBTAG00000019291	−3.03	$4.98E^{-05}$
TRIM7	ENSBTAG00000020954	−3.29	$8.57E^{-06}$
DUS4L	ENSBTAG00000021849	−2.90	$7.65E^{-05}$
ECSCR	ENSBTAG00000030518	−3.29	$5.01E^{-06}$
LOC112448304	ENSBTAG00000042475	−1.48	$5.16E^{-05}$
NA	ENSBTAG00000056594	−3.47	$1.35E^{-06}$
NA	ENSBTAG00000059357	−1.54	$3.31E^{-05}$
NA	ENSBTAG00000063983	−2.97	$6.39E^{-05}$
TLR1	ENSBTAG00000064150	−2.96	$5.15E^{-05}$
NA	ENSBTAG00000067673	−3.52	$1.32E^{-06}$
NA	ENSBTAG00000069885	−2.17	$1.57E^{-07}$
NA	ENSBTAG00000073706	−3.08	$2.85E^{-05}$
5S_rRNA	ENSBTAG00000076020	−3.24	$1.52E^{-06}$

NA Not Applicable

Results of screening the hub targets

The PPI network of 403 potential targets was constructed via the STRING database and visualized with Cytoscape v3.10.2 software (Fig. 5). This network contains 259 nodes and 540 edges, with an average node degree of 3.16 and a PPI enrichment *p* value of $< 1.0e^{-16}$.

A total of 12 gene clusters were obtained via the MCODE plugin (Supplementary Table 4). Through comprehensive analysis of five algorithms (MCC, MNC, degree, betweenness centrality, and closeness centrality) of the CytoHubba plugin, 4 hub genes (PRKACA, PRKCB, IL6, and MAPK1) were identified (Fig. 6A ~ F). These targets, together with the 4 aforementioned DEGs, constitute the 8 hub targets identified in this study. To our knowledge, these 8 hub targets play a vital role in reproduction or metabolism. For example, MMP2 is a key regulatory factor of the extracellular matrix (ECM), MAPK1 is involved in regulating cell proliferation and apoptosis, PRKCB regulates cell proliferation, apoptosis, and metabolism, and PRKACA modulates oocyte meiosis.

Results of the GO and KEGG enrichment analyses

The bubble plot (Fig. 7A) revealed the top 10 most enriched GO terms for 403 potential targets. The lollipop plot (Fig. 7B) revealed the top 30 most enriched KEGG pathways for 403 potential targets. The Sankey–Lollipop

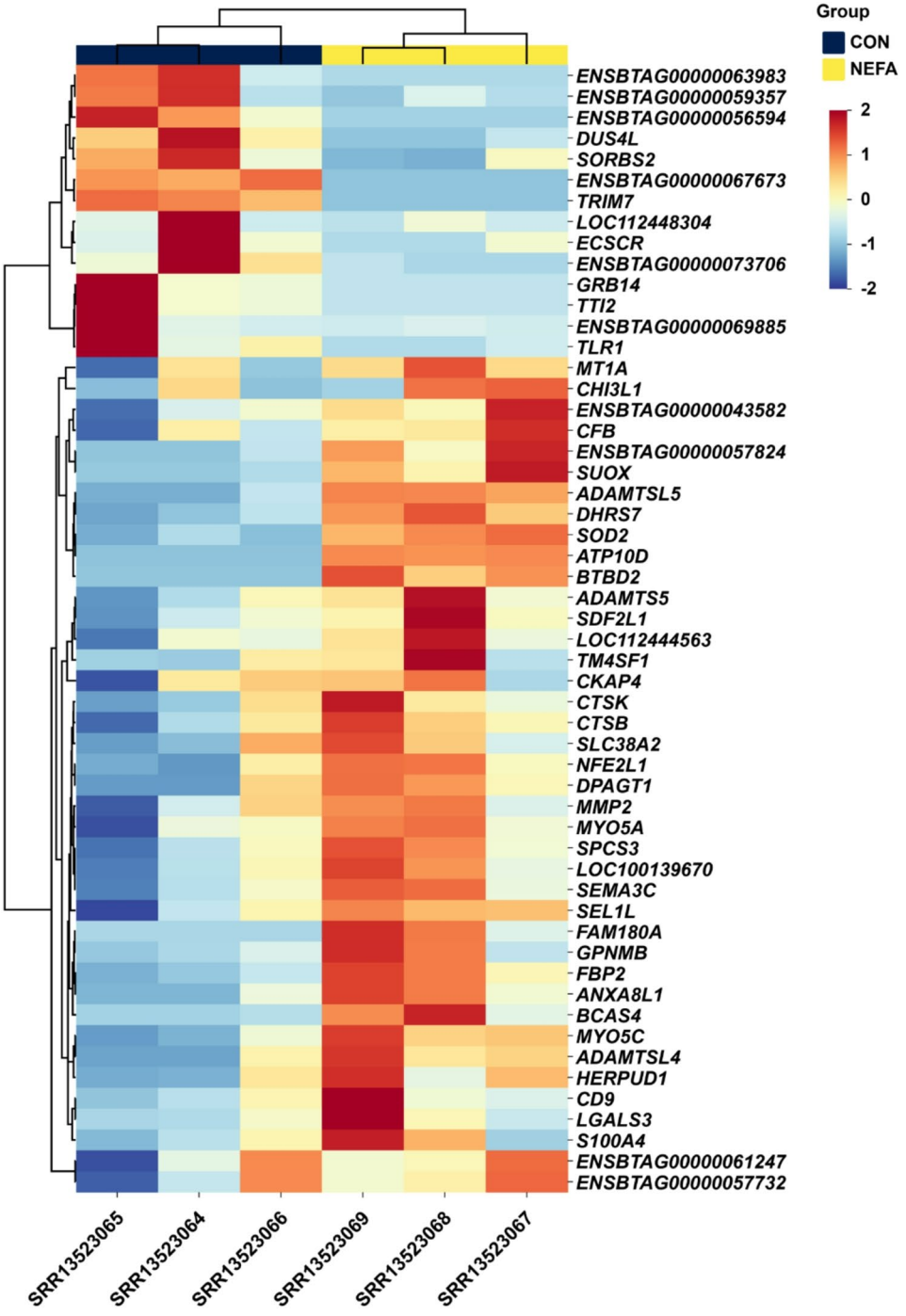

Fig. 3 Heatmap of intragroup consistency analysis of the DEGs. The gene name is represented by an official symbol, and the gene without an official symbol is replaced by an Ensembl ID

plot (Fig. 7C) revealed the 11 most significantly enriched KEGG pathways for the 8 hub targets. All the above rankings are sorted by ascending FDR values.

The GO enrichment analysis of 403 potential targets revealed 229 biological process (BP), 24 cellular component (CC) and 47 molecular function (MF) terms; the KEGG enrichment analysis revealed 201 potential pathways (Supplementary Table 5). GO enrichment analysis (Fig. 7A; Supplementary Table 5) revealed that BPs were involved mainly in metabolic regulation, physiological homeostasis and other related pathways; CCs were involved mainly in pathways related to membrane signal transduction and neuronal function; and MFs were involved mainly in biological processes such as enzyme

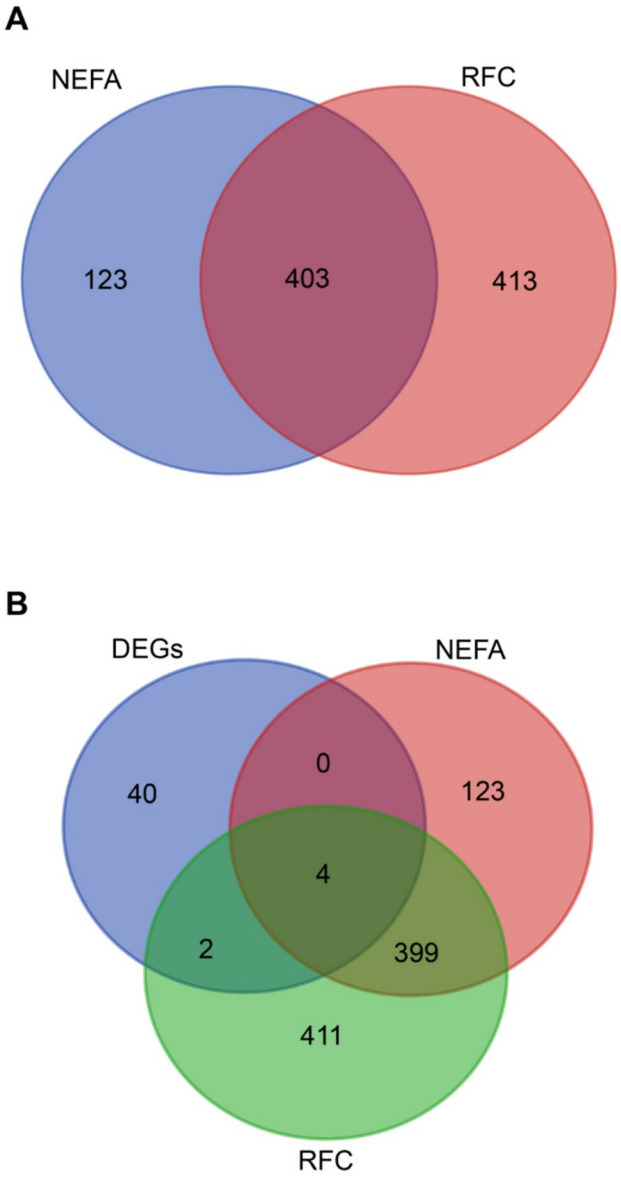

Fig. 4 Cross-analysis of target sets. **A** Cross-analysis of the NEFA and RFC target sets. **B** Cross-analysis of DEGs, NEFAs and RFC target sets

catalysis, molecular binding, and transport. KEGG enrichment analysis (Fig. 7B; Supplementary Table 5) revealed that the AGE-RAGE signaling pathway in diabetic complications, lipids and atherosclerosis, proteoglycans in cancer, and the HIF-1 signaling pathway were the most significantly enriched pathways. These pathways can influence lipid metabolism, as well as germ cell development, fertilization, or pregnancy. For example, the AGE-RAGE signaling pathway in diabetic complications promotes lipid deposition and impairs germ cell function, and the HIF-1 signaling pathway maintains lipid metabolic homeostasis and regulates germ cell maturation, suggesting their potential significance in the regulatory mechanism and development of NEFA-induced RFC toxicity.

The GO enrichment analysis of MCODE cluster 1 (Table 4) is shown in Fig. 7D, and the genes of this module were involved mainly in the biological process of the steroid hormone signaling pathway, which includes key processes: hormone signaling and cellular communication, kinase signaling hubs, hormone signaling perception, and activation and transcriptional regulation.

KEGG enrichment analysis of the hub genes (Fig. 7C) revealed that the GnRH signaling pathway and the AGE-RAGE signaling pathway in diabetic complications were the most significantly enriched pathways associated with the genes, indicating that reproductive hormones and advanced glycation end products (AGEs) may play a vital role in NEFA-induced RFC toxicity.

In addition, the KEGG pathways of the 403 potential targets and 8 hub targets highly and significantly overlapped, underscoring the pivotal role of the 8 hub targets among the 403 potential targets (Fig. 7E; Supplementary Table 6).

Results of molecular Docking

The molecular docking results (Fig. 8 A) revealed that the binding energies of MMP2, MAPK1, PRKACA and PRKCB to NEFAs were all < -5.0 kcal/mol, suggesting that these proteins can spontaneously bind to NEFAs and indicate thermodynamically favorable and stable binding interactions. Further analysis revealed that NEFAs formed hydrogen bonds with these four target proteins (Fig. 8B ~ E), further emphasizing the strong binding affinity between these targets and NEFAs. These findings validate and underscore the critical role of these targets in the molecular mechanism of NEFA-induced RFC toxicity.

Discussion

This study provides the first integrative toxicological framework combining network toxicology, transcriptomics, and molecular docking to elucidate the molecular mechanisms by which NEFAs contribute to reduced fertility in dairy cows. Our findings indicate that NEFAs can induce inflammatory responses, signaling pathway dysregulation, and lipid metabolic imbalance via the combined effects of multiple signaling pathways and metabolic networks, ultimately impairing ovarian function and hormonal homeostasis. This study not only provides a novel toxicological perspective for understanding the link between metabolic stress and reproductive disorders but also lays a theoretical foundation for future molecular intervention strategies to increase dairy cow reproductive performance.

High circulating concentrations of NEFAs, although normal metabolites of cows in the NEB state, are thought

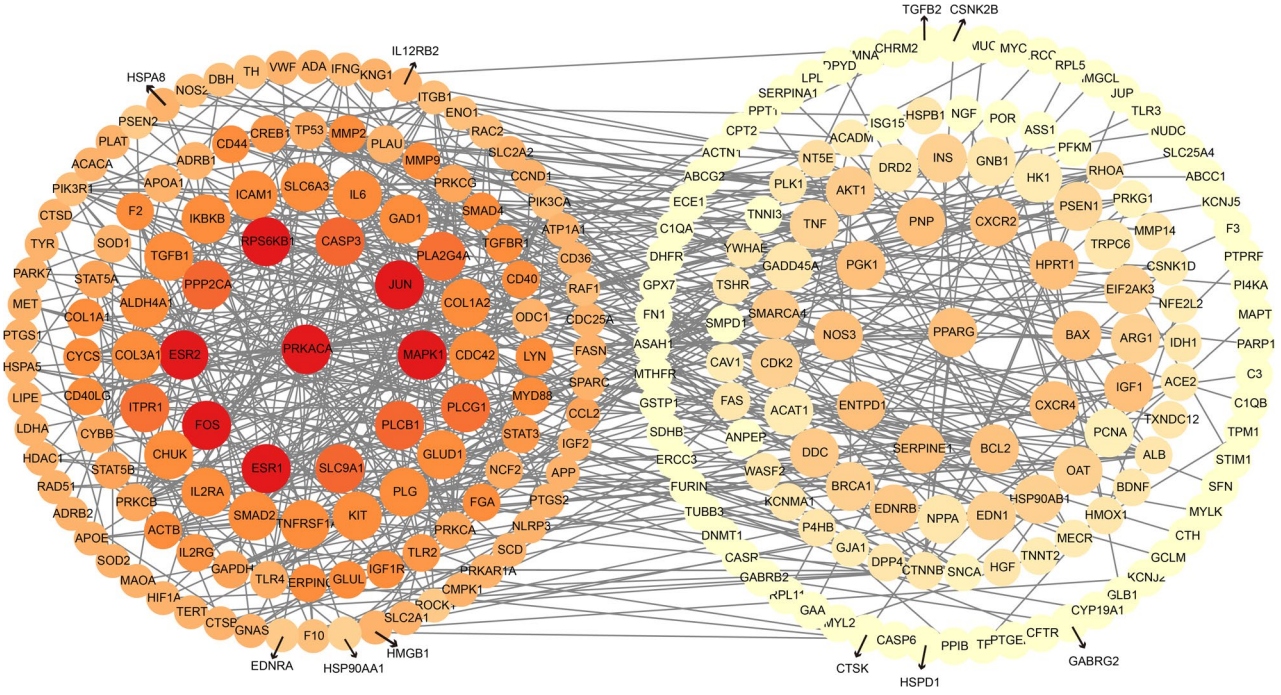

Fig. 5 PPI network of the 403 potential targets shared between the NEFA and RFC target sets. Nodes are colored and sized according to their MCODE score, with darker colors indicating higher MCODE scores

to be strongly associated with endocrine disorders, immune dysfunction, and metabolic imbalances in dairy cows, which contribute to the development of diseases such as reproductive diseases, ketosis, gastric shift, and fatty liver syndrome. Furthermore, the occurrence of these diseases may in turn induce more severe endocrine, immune, and metabolic issues, thereby initiating a vicious cycle [3, 4, 18]. For example, high concentrations of NEFAs inhibit insulin secretion and downregulate insulin-like growth factor-1 (IGF-1) synthesis, thereby impairing follicular development and promoting cystic follicle formation. This induces ovarian dysfunction, leading to persistent estrogen deficiency. Since estrogen normally inhibits the promoting effect of proliferator-activated receptor α (PPARα) in lipid metabolism, this estrogen deficiency results in dysregulated lipid metabolism—ultimately enhancing lipid mobilization and further increasing NEFA levels [19–21]. Once the rate of NEFA production exceeds that of PPARα-mediated fatty acid breakdown, excess NEFAs may accumulate in the form of triglycerides, thereby causing cellular damage and diseases. In addition, high concentrations of NEFAs attract monocytes to infiltrate endometrial tissue, which promotes the release of inflammatory factors and induces local inflammation of the endometrium. This inhibits its DMI in dairy cows, leading to more severe NEB and increased NEFA production [4, 19, 22, 23].

Several studies have demonstrated that exposure to high concentrations of NEFAs is positively correlated with the development of inflammation [7, 24, 25], suggesting that inflammatory responses may serve as a key pathway mediating NEFA-induced reproductive toxicity. Our analysis revealed significant upregulation of genes such as SOD2 and MMP2 under high NEFA exposure (Table 2). These genes play core roles in oxidative stress and inflammatory responses, particularly MMP2, which is a common target for both NEFAs and RFC. MMP2 is a member of the matrix metalloproteinase family, and its main function is to participate in the remodeling and degradation of the ECM [26]. The ECM is tightly regulated by proteins such as MMP2, and disruption of this regulatory balance may lead to abnormal embryonic implantation or infertility [27]. Previous studies have shown that the mRNA and protein levels of MMP2 are significantly increased in a bovine endometritis model induced by *Escherichia coli* and *Staphylococcus aureus* [28]. Therefore, high concentrations of NEFAs may induce the dysregulation of genes such as MMP2 and SOD2, increase oxidative stress and local inflammation, and ultimately contribute to reproductive toxicity in dairy cows.

In addition, the AGE-RAGE signaling pathway in diabetic complications, which was the most significantly enriched pathway in the KEGG enrichment analysis of potential targets and hub targets. The identification of the AGE-RAGE signaling pathway as a central mechanism in NEFA-induced RFC is particularly novel, suggesting a previously underappreciated link between metabolic stress and reproductive inflammation. AGEs may be key

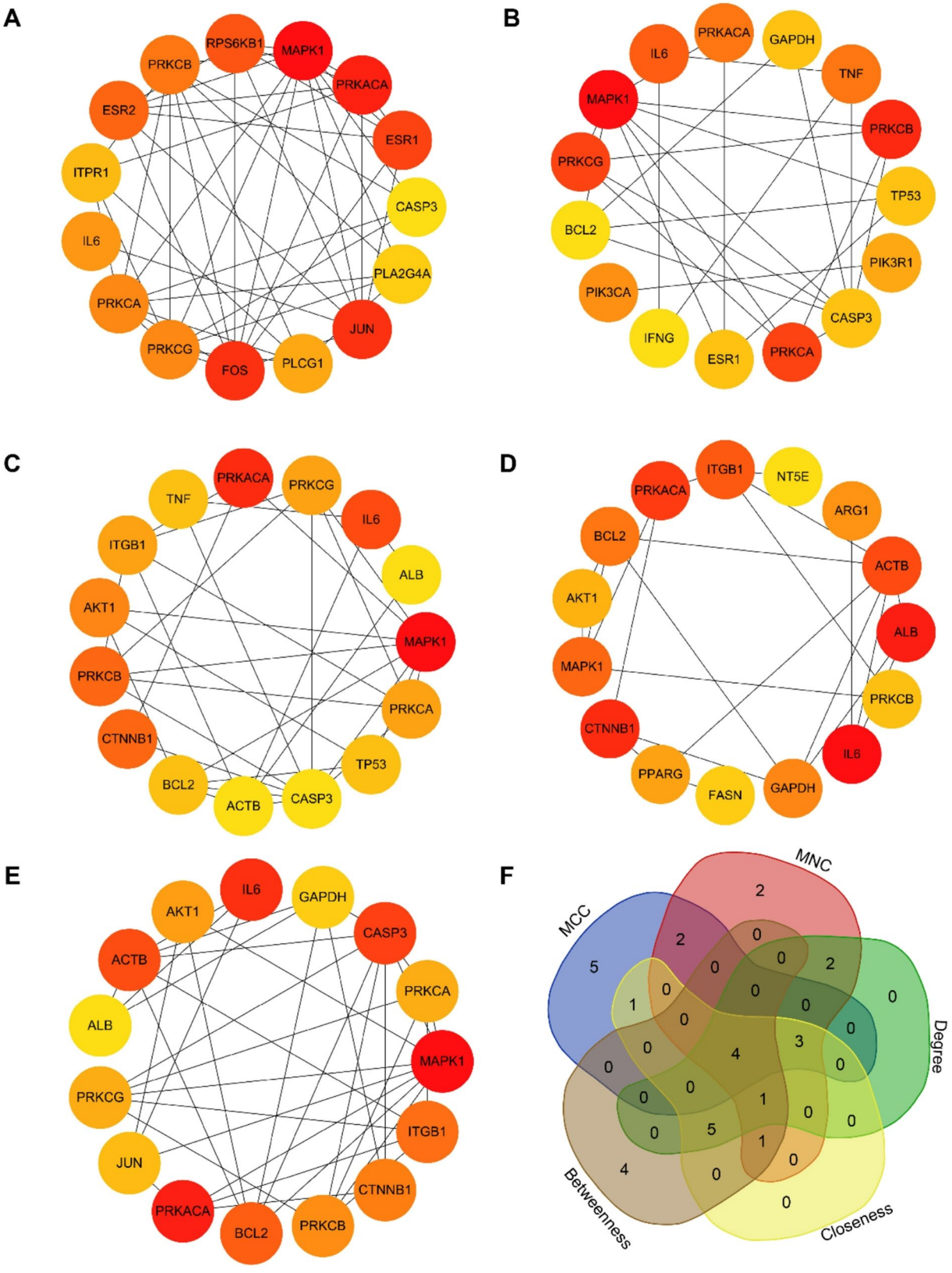

Fig. 6 The top 15 targets and cross-analysis of the PPI network via the MCC, MNC, degree, betweenness centrality and closeness centrality algorithms. **A** The top 15 targets of the PPI network via the MCC algorithm. **B** The top 15 targets of the PPI network via the MNC algorithm. **C** The top 15 targets of the PPI network via the degree algorithm. **D** The top 15 targets of the PPI network via the betweenness centrality algorithm. **E** The top 15 targets of the PPI network via the closeness centrality algorithm. **F** Cross-analysis of the top 15 targets via five algorithms

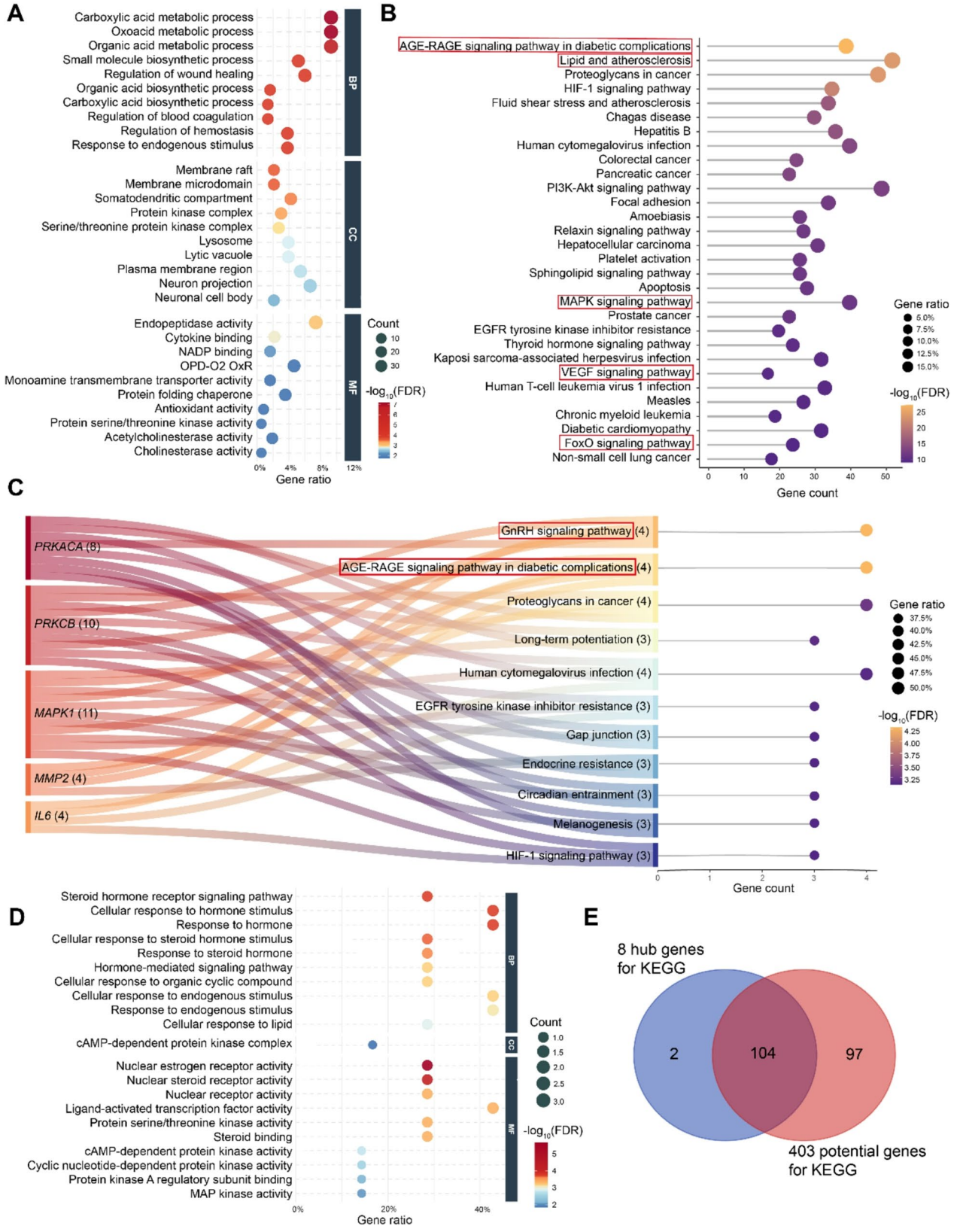

Fig. 7 GO and KEGG enrichment analyses of 403 potential targets, 8 hub targets and MCODE cluster 1. **A** Bubble plot of the results of the GO enrichment analysis of 403 potential targets. **B** Lollipop plot of the results of the KEGG enrichment analysis of 403 potential targets. **C** Sankey–Lollipop plot of the top 11 enriched genes identified via KEGG analysis of the 8 hub targets. **D** Bubble plot of the GO enrichment analysis of MCODE cluster 1. **E** Cross-analysis of KEGG enrichment results between 8 hub targets and 403 potential targets

Table 4 Information on MCODE cluster 1

MCODE clusters	Targets	MCODE node status	MCODE score	Closeness centrality	Betweenness centrality	Degree
Cluster 1	ESR2	Seed	6.0	0.28	0.00	6
	ESR1	Clustered	6.0	0.31	0.03	12
	FOS	Clustered	6.0	0.29	0.00	9
	JUN	Clustered	6.0	0.32	0.03	11
	MAPK1	Clustered	6.0	0.33	0.10	26
	PRKACA	Clustered	6.0	0.33	0.11	24
	RPS6KB1	Clustered	6.0	0.29	0.00	8

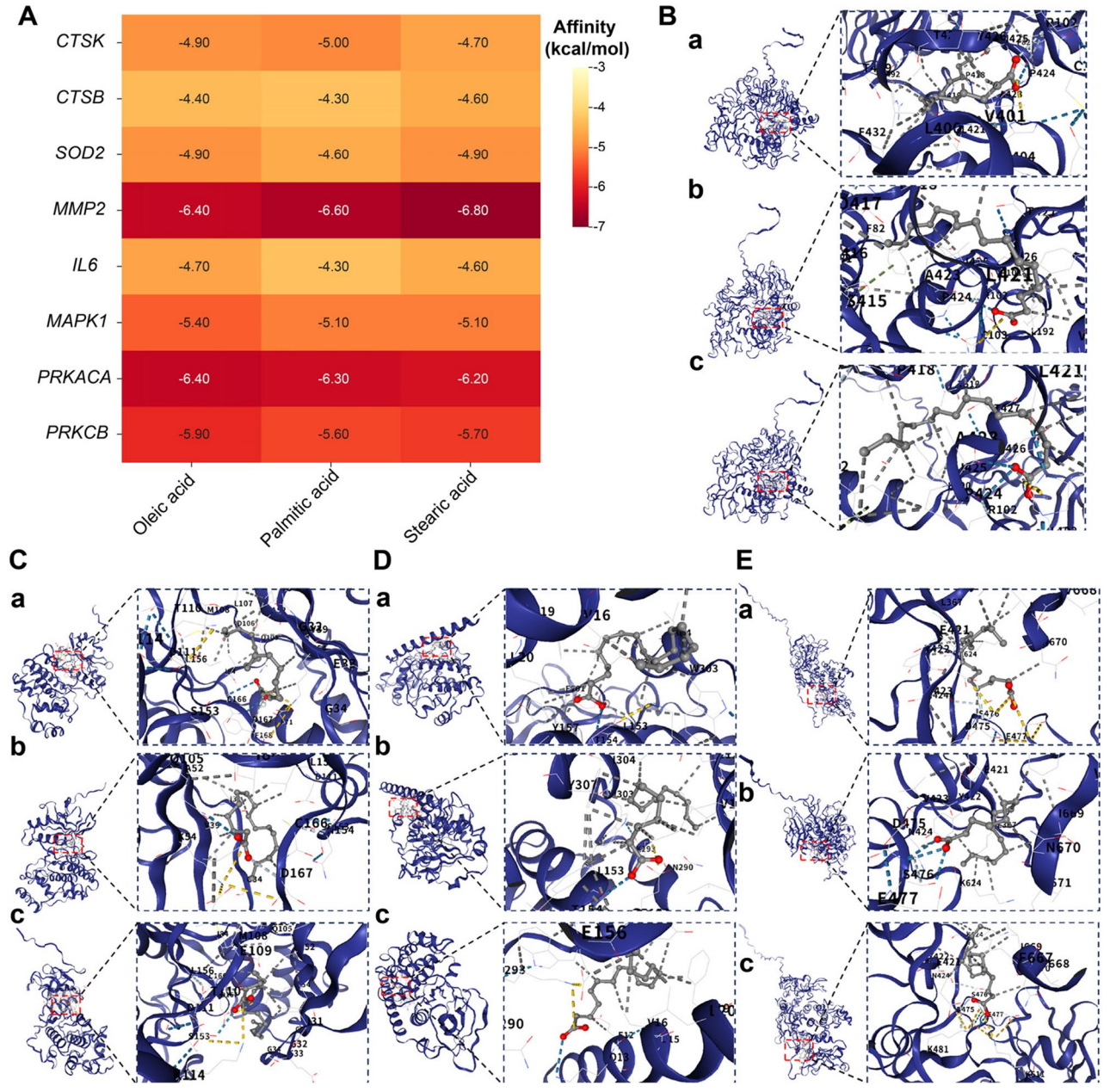

Fig. 8 The binding energy and visual results of molecular docking. **A** Heatmap of the molecular docking affinity of 8 hub targets and NEFAs (OA, PA and SA). **B** Molecular docking visualization of MMP2 with NEFAs. **C** Molecular docking visualization of MAPK1 with NEFAs. **D** Molecular docking visualization of PRKACA with NEFAs. **E** Molecular docking visualization of PRKCB with NEFAs. In figures B~E, "a", "b", and "c" indicate OA, PA and SA, respectively; connecting lines with yellow, blue, pale blue and gray indicate ionic interactions, hydrogen bonds, weak hydrogen bonds, and hydrophobic contacts, respectively

factors in the pathological development of NEFA-mediated RFC toxicity. AGEs are irreversible products formed through nonenzymatic reactions between reducing sugars and molecules such as proteins, lipids, and nucleic acids [29]. Studies have demonstrated that AGEs may exacerbate endothelial dysfunction, infertility, endometritis, and oxidative stress in ovarian cells [29–31]. The binding of AGEs to the RAGE receptor induces mitogen-activated protein kinases (MAPKs) upregulation by activating key transcription factors such as NF-κB and AP-1, which subsequently induce the expression of proinflammatory genes such as IL-1β, IL-6, and TNF-α, ultimately exacerbating the inflammatory response and oxidative stress [29]. In this study, NEFAs may promote the production and accumulation of AGEs, exacerbating inflammatory responses and oxidative stress through AGE/RAGE/MAPK cascade reactions and ultimately promoting the development of RFC.

Our results indicate that abnormalities in the MAPK/protein kinase A (PKA) signaling pathway may play a significant role in NEFA-mediated reproductive toxicity. MAPKs and cyclic adenosine monophosphate (cAMP)-dependent PKA are involved in the regulation of oocyte maturation [32, 33]. MAPK1, a key member of the MAPK family, can be activated by various cytokines, growth factors, reactive oxygen species, and high glucose to promote cell differentiation, proliferation, growth, and apoptosis [34, 35]. MAPK1 also synergizes with maturation-promoting factors in the regulation of bovine oocyte maturation [36]. PRKACA, the major catalytic subunit of PKA, can arrest meiosis resumption in bovine oocytes [33]. PRKACA is also related to the follicle-stimulating hormone-induced proliferation of granulosa cells [37]. Investigating the underlying association between NEFA exposure and the dysregulation of MAPK1 or PRKACA could help elucidate the molecular mechanisms underlying NEFA-mediated RFC.

In addition to MAPK1 and PRKACA, PRKCB emerged as a notable hub gene with potential links to metabolic and reproductive dysfunction. PRKCB is a key member of the protein kinase C (PKC) family, encoding PKC-β, which is dependent on calcium ions and diacylglycerol for its phosphorylation to regulate cell proliferation, apoptosis, and metabolism [38]. Notably, PRKCB is a key regulatory gene for diabetes and its complications [38, 39], and high concentrations of NEFAs are closely associated with dairy cow ketosis (a major complication of diabetes) [40]. This may serve as a link between metabolic disorders and reproductive dysfunction. Therefore, exploring the relationship between high levels of NEFAs and PRKCB expression could further refine and elucidate the mechanism of RFC toxicity caused by NEFAs.

GO and KEGG pathway enrichment analyses revealed the pathways that may be affected by NEFA exposure and the molecular processes involved in the progression of RFC, thereby enabling a deeper understanding of the biological mechanisms underlying NEFA exposure leading to RFC. The combined GO and KEGG enrichment analyses of 403 potential targets and 8 hub targets suggested that NEFAs may affect RFC through multiple pathways, including the AGE-RAGE signaling pathway in diabetic complications, the GnRH signaling pathway, lipid metabolism disorders, apoptosis, the MAPK signaling pathway, the VEGF signaling pathway, and the FoxO signaling pathway. These pathways are involved in key processes, including hormone regulation, inflammation, oxidative stress, angiogenesis, tissue remodeling, apoptosis, cell survival and energy metabolism. In addition, the GO enrichment analysis of MCODE cluster 1, the highest-scoring gene cluster via the MCODE method, involved mainly the steroid hormone signaling pathway. These findings suggest that NEFAs may disrupt the complex endocrine-immune-metabolic network, leading to hormonal disturbances, inflammatory responses, and lipid metabolism imbalances, which in turn cause reproductive toxicity in dairy cows.

We performed PCA to assess the overall variation and distribution of gene expression data between the normal (CON) and NEFA groups. The PCA results did not show clear separation between groups, which may be due to the limited sample size (n = 3 per group) and the inherent biological variability of the tissue samples. However, PCA has limitations in identifying transcriptional differences: as an unsupervised method, PCA can identify directions that explain the maximum variance in high-dimensional datasets, but such separation relies on global gene expression rather than individual genes; even though PCA captures an overall trend of variance, it does not yield specific DEGs [41–43]. Therefore, the lack of clear separation in PCA does not imply the absence of biological differences. The interpretation of the PCA results should be combined with subsequent analysis of the DEGs, enrichment analysis, etc [44]. In this study, even though the PCA results were unsatisfactory, on the basis of the hierarchical clustering of DEGs (Fig. 3) and enrichment analyses (Fig. 6C and E), the DEG group exhibited a consistent trend of gene expression, and the enrichment analyses revealed RFC-associated pathways, including the AGE-RAGE signaling pathway in diabetic complications and the GnRH signaling pathway. In addition, we performed hierarchical clustering based on all expressed genes (Supplementary Fig. 1), which also exhibited partial yet less distinct group separation—consistent with the PCA results. Together, these analyses indicate that while overall transcriptomic variance was modest, biologically relevant differential expression signals were captured at the DEG level.

In this study, we prioritized MMP2, MAPK1, PRKACA, and PRKCB as hub targets based on several methodological considerations. First, although the GSE165476 dataset provided experimentally supported transcriptomic responses, among the four DEG-derived hub targets (MMP2, CTSB, CTSK, and SOD2), only MMP2 passed molecular docking validation (< – 5.0 kcal/mol), indicating its reliable direct interaction with NEFAs (Fig. 8). Second, to predict a comprehensive landscape of NEFA-mediated RFC toxicity, we applied multiple CytoHubba algorithms to the PPI network constructed from the 403 overlapping genes (Fig. 6). This multi-algorithm integration strategy identified four top-ranking hub genes—PRKACA, PRKCB, IL6, and MAPK1—across multiple topological metrics. These algorithms capture critical nodes from the perspectives of network structure, information flow, and centrality. Among these, PRKACA, PRKCB, and MAPK1 confirmed potential interactions with NEFAs through molecular docking (Fig. 8), whereas IL6 was excluded from the prioritized list as it failed to pass docking validation. This integrative strategy not only highlights transcriptomic evidence but also expands the predictive capacity of network toxicology to uncover potential regulatory mechanisms. Although some non-DEG hub targets lack direct transcriptional support, they may represent upstream signaling regulators or indirect effectors, thereby providing a hypothetical basis for subsequent experimental validation.

In conclusion, although this study provides novel insights into the toxicological mechanisms underlying NEFA-mediated fertility reduction in dairy cows, it has several limitations. First, all analyses relied on in silico predictions and a publicly available transcriptomic dataset (GSE165476), thereby introducing potential confounding factors due to the inability to control experimental conditions. Second, the absence of in vitro or in vivo validation constrains the direct biological and translational relevance of the findings. Future studies should prioritize the validation of the expression of hub genes such as MMP2, MAPK1, PRKACA, and PRKCB via qPCR and Western blotting in NEFA-exposed bovine ovarian or granulosa cell models. These experiments will serve to confirm the regulatory roles of these genes and pathways in NEFA-induced reproductive toxicity. Furthermore, subsequent studies should explore systemic metabolic interactions involving endocrine and immune responses during NEFA exposure. Integrating these experimental data with in silico predictions from this study will contribute to a more comprehensive elucidation of NEFA-induced reproductive toxicity.

Conclusions

This study is the first to integrate network toxicology, transcriptomics, and molecular docking approaches to systematically explore the potential molecular mechanisms of the endogenous metabolite NEFA-mediated RFC. By integrating these three approaches, we established a complete systematic chain of screening-prediction-verification, which not only advances the understanding of NEFA-mediated reproductive toxicity but also provides potential biomarkers and molecular targets for improving reproductive management strategies in dairy cows. Future studies should focus on animal and cell modeling experiments, multiomics studies, endocrine–immune–metabolic networks and molecular dynamics simulations to explore and validate the potential effects of these targets on RFC across multiple levels. These studies provide deeper and more comprehensive insights into targeting the inhibition of NEFA toxicity to RFC to ultimately improve reproductive performance and reduce culling rates in dairy cows.

Abbreviations

NEFAs	Nonesterified fatty acids
NEB	Negative energy balance
RFC	Reduced fertility in cows
GO	Gene Ontology
KEGG	Kyoto Encyclopedia of Genes and Genomes
OA	Oleic acid
PA	Palmitic acid
SA	Stearic acid
DEGs	Differentially expressed genes
SMILES	Simplified molecular input line entry system
PPARγ	Proliferator-activated receptor γ
PPI	Protein–protein interaction
MCODE	Molecular Complex Detection
MCC	Maximum clique centrality
MNC	Maximum neighborhood component
PCA	Principal component analysis
FDR	False discovery rate
ECM	Extracellular matrix
BP	Biological process
CC	Cellular component
MF	Molecular function
AGEs	Advanced glycation end products
PPARα	Proliferator-activated receptor α
MAPKs	Mitogen-activated protein kinases
cAMP	cyclic adenosine monophosphate
PKC	Protein kinase C

Supplementary Information

The online version contains supplementary material available at https://doi.org/10.1186/s12864-025-12444-6.

Supplementary Material 1.

Supplementary Material 2.

Supplementary Material 3.

Supplementary Material 4.

Supplementary Material 5.

Supplementary Material 6.

Supplementary Material 7.

Supplementary Material 8.

Acknowledgements
Not applicable.

Authors' contributions
JW: Conceptualization, Investigation, Formal analysis, Software, Visualization, Writing–original draft. WW: Methodology, Validation, Writing–review & editing. XK: Formal analysis, Visualization, Writing–review & editing. YL: Software, Formal analysis, Writing–review & editing. LL: Methodology, Supervision, Writing–review & editing. YL: Funding acquisition, Supervision, Writing–review & editing. HH: Funding acquisition, Project administration, Supervision, Writing–review & editing. All the authors have read and approved the final version of the manuscript.

Funding
This work was financially supported by grants from the Science and Technology Department of Xinjiang Uygur Autonomous Region (2024AB034) and the National Key Research and Development Program of China (2023YFE0107600).

Data availability
The datasets presented in this study can be found in online repositories. The names of the repository/repositories and accession number(s) can be found in the article/supplementary material. All other data generated or analyzed during this study are provided in the supplementary material.

Declarations

Ethics approval and consent to participate
Not applicable.

Consent for publication
Not applicable.

Competing interests
The authors declare no competing interests.

Received: 3 September 2025 / Accepted: 15 December 2025
Published online: 29 January 2026

References

1. Khemarach S, Yammuen-art S, Punyapornwithaya V, Nithithanasilp S, Jaipolsaen N, Sangsritavong S. Improved reproductive performance achieved in tropical dairy cows by dietary beta-carotene supplementation. Sci Rep. 2021;11:23171. https://doi.org/10.1038/s41598-021-02655-8.
2. Tufarelli V, Puvača N, Glamočić D, Pugliese G, Colonna MA. The most important metabolic diseases in dairy cattle during the transition period. Animals-basel. 2024;14:816. https://doi.org/10.3390/ani14050816.
3. Mezzetti M, Cattaneo L, Passamonti MM, Lopreiato V, Minuti A, Trevisi E. The transition period updated: a review of the new insights into the adaptation of dairy cows to the new lactation. Dairy. 2021;2:617–36. https://doi.org/10.3390/dairy2040048.
4. Adewuyi AA, Gruys E, Van Eerdenburg FJCM. Non esterified fatty acids (NEFA) in dairy cattle. A review. Vet Q. 2005;27:117–26. https://doi.org/10.1080/01652176.2005.9695192.
5. Pedroza GH, Lanzon LF, Rabaglino MB, Walker WL, Vahmani P, Denicol AC. Exposure to non-esterified fatty acids in vitro results in changes in the ovarian and follicular environment in cattle. Anim Reprod Sci. 2022;238:106937. https://doi.org/10.1016/j.anireprosci.2022.106937.
6. Ribeiro ES, Lima FS, Greco LF, Bisinotto RS, Monteiro APA, Favoreto M, et al. Prevalence of periparturient diseases and effects on fertility of seasonally calving grazing dairy cows supplemented with concentrates. J Dairy Sci. 2013;96:5682–97. https://doi.org/10.3168/jds.2012-6335.
7. Kaneene JB, Miller R, Herdt TH, Gardiner JC. The association of serum non-esterified fatty acids and cholesterol, management and feeding practices with peripartum disease in dairy cows. Prev Vet Med. 1997;31:59–72. https://doi.org/10.1016/s0167-5877(96)01141-5.
8. Macmillan K, Gobikrushanth M, Helguera IL, Behrouzi A, Colazo MG. Relationships between early postpartum nutritional and metabolic profiles and subsequent reproductive performance of lactating dairy cows. Theriogenology. 2020;151:52–7. https://doi.org/10.1016/j.theriogenology.2020.03.034.
9. Lüttgenau J, Purschke S, Tsousis G, Bruckmaier RM, Bollwein H. Body condition loss and increased serum levels of nonesterified fatty acids enhance progesterone levels at estrus and reduce estrous activity and insemination rates in postpartum dairy cows. Theriogenology. 2016;85:656–63. https://doi.org/10.1016/j.theriogenology.2015.10.003.
10. Cardoso FC, LeBlanc SJ, Murphy MR, Drackley JK. Prepartum nutritional strategy affects reproductive performance in dairy cows. J Dairy Sci. 2013;96:5859–71. https://doi.org/10.3168/jds.2013-6759.
11. Leroy JLMR, Vanholder T, Mateusen B, Christophe A, Opsomer G, De Kruif A, et al. Non-esterified fatty acids in follicular fluid of dairy cows and their effect on developmental capacity of bovine oocytes in vitro. Reproduction. 2005;130:485–95. https://doi.org/10.1530/rep.1.00735.
12. Van Hoeck V, Sturmey RG, Bermejo-Alvarez P, Rizos D, Gutierrez-Adan A, Leese HJ, et al. Elevated non-esterified fatty acid concentrations during bovine oocyte maturation compromise early embryo physiology. PLoS One. 2011;6:e23183. https://doi.org/10.1371/journal.pone.0023183.
13. Zhang X, Fan H, Li Y, Xiao X, Liu R, Qi J, et al. Development and application of network toxicology in safety research of Chinese materia medica. Chin Herb Med. 2015;7:27–38. https://doi.org/10.1016/S1674-6384(15)60016-8.
14. Tripathi SK, Muttineni R, Singh SK. Extra precision docking, free energy calculation and molecular dynamics simulation studies of CDK2 inhibitors. J Theor Biol. 2013;334:87–100. https://doi.org/10.1016/j.jtbi.2013.05.014.
15. Minge CE, Robker RL, Norman RJ. PPAR gamma: coordinating metabolic and immune contributions to female fertility. PPAR Res. 2008;2008:243791. https://doi.org/10.1155/2008/243791.
16. Li Y, Zhou T, Liu Z, Zhu X, Wu Q, Meng C, et al. Air pollution and prostate cancer: unraveling the connection through network toxicology and machine learning. Ecotoxicol Environ Saf. 2025;292:117966. https://doi.org/10.1016/j.ecoenv.2025.117966.
17. Liu Y, Yang X, Gan J, Chen S, Xiao Z-X, Cao Y. CB-Dock2: improved protein–ligand blind docking by integrating cavity detection, docking and homologous template fitting. Nucleic Acids Res. 2022;50:W159-64. https://doi.org/10.1093/nar/gkac394.
18. Kia S, Mohri M, Seifi HA. Association of precalving serum NEFA concentrations with postpartum diseases and reproductive performance in multiparous Holstein cows: cut-off values. Vet Med Sci. 2023;9:1757–63. https://doi.org/10.1002/vms3.1143.
19. Vanholder T, Opsomer G, de Kruif A. Aetiology and pathogenesis of cystic ovarian follicles in dairy cattle: a review. Reprod Nutr Dev. 2006;46:105–19. https://doi.org/10.1051/rnd:2006003.
20. Yoon M. The role of PPARα in lipid metabolism and obesity: focusing on the effects of estrogen on PPARα actions. Pharmacol Res. 2009;60:151–9. https://doi.org/10.1016/j.phrs.2009.02.004.
21. Pawlak M, Lefebvre P, Staels B. Molecular mechanism of PPARα action and its impact on lipid metabolism, inflammation and fibrosis in non-alcoholic fatty liver disease. J Hepatol. 2015;62:720–33. https://doi.org/10.1016/j.jhep.2014.10.039.
22. Van Hoeck V, Bols PEJ, Binelli M, Leroy JLMR. Reduced oocyte and embryo quality in response to elevated non-esterified fatty acid concentrations: a possible pathway to subfertility? Anim Reprod Sci. 2014;149:19–29. https://doi.org/10.1016/j.anireprosci.2014.07.015.
23. Wathes DC, Clempson AM, Pollott GE. Associations between lipid metabolism and fertility in the dairy cow. Reprod Fertil Dev. 2012;25:48–61. https://doi.org/10.1071/RD12272.
24. Wen Y, Wang Y, Loor JJ, Zhao C, Wang J. Non-esterified fatty acids disrupt hepatic lipid metabolism and mitochondrial function via TLR4/MyD88/IRAK2 signaling in bovine hepatocytes. J Steroid Biochem Mol Biol. 2025;253:106813. https://doi.org/10.1016/j.jsbmb.2025.106813.
25. Wang Y, Li C, Ali I, Li L, Wang G. N-acetylcysteine modulates non-esterified fatty acid-induced pyroptosis and inflammation in granulosa cells. Mol Immunol. 2020;127:157–63. https://doi.org/10.1016/j.molimm.2020.09.011.
26. Ramu D, Venkatesan V, Paul SFD, Koshy T. Genetic variation in matrix metalloproteinase MMP2 and MMP9 as a risk factor for idiopathic recurrent spontaneous abortions in an Indian population. J Assist Reprod Genet. 2017;34:945–9. https://doi.org/10.1007/s10815-017-0939-x.

27. Grötter LG, Cainelli S, Peralta MB, Angeli E, Belotti EM, Ortega HH, et al. Metalloproteases and their inhibitors in the postpartum endometrial remodeling in dairy cows: their relationship with days to conception after parturition. Vet Res Commun. 2025;49:53. https://doi.org/10.1007/s11259-024-10622-7.
28. Wu J, Bai F, Mao W, Liu B, Yang X, Zhang J, et al. Anti-inflammatory effects of the prostaglandin D2/prostaglandin DP1 receptor and lipocalin-type prostaglandin D2 synthase/prostaglandin D2 pathways in bacteria-induced bovine endometrial tissue. Vet Res. 2022;53:98. https://doi.org/10.1186/s13567-022-01100-6.
29. Adamopoulos C, Piperi C, Gargalionis AN, Dalagiorgou G, Spilioti E, Korkolopoulou P, et al. Advanced glycation end products upregulate lysyl oxidase and endothelin-1 in human aortic endothelial cells via parallel activation of ERK1/2–NF-κB and JNK–AP-1 signaling pathways. Cell Mol Life Sci. 2016;73:1685–98. https://doi.org/10.1007/s00018-015-2091-z.
30. Li Q, Cao Zh, Ling X, Sun P, Yin W, Fan K, et al. Potential molecular targets and pathways of a traditional Chinese medicine formula for bovine endometritis identified by network pharmacology. Pol J Vet Sci. 2024;27:363–77. https://doi.org/10.24425/pjvs.2024.151730.
31. Twarda-Clapa A, Olczak A, Białkowska AM, Koziołkiewicz M. Advanced glycation end-products (AGEs): formation, chemistry, classification, receptors, and diseases related to ages. Cells. 2022;11:1312. https://doi.org/10.3390/cells11081312.
32. Marei WF, Wathes DC, Fouladi-Nashta AA. Impact of linoleic acid on bovine oocyte maturation and embryo development. Reproduction. 2010;139:979–88. https://doi.org/10.1530/REP-09-0503.
33. Bernal-Ulloa SM, Heinzmann J, Herrmann D, Hadeler K-G, Aldag P, Winkler S, et al. Cyclic AMP affects oocyte maturation and embryo development in prepubertal and adult cattle. PLoS One. 2016;11:e0150264. https://doi.org/10.1371/journal.pone.0150264.
34. Tian W, Zhang Z, Cohen DM. MAPK signaling and the kidney. Am J Physiol Renal Physiol. 2000;279:F593-604. https://doi.org/10.1152/ajprenal.2000.279.4.F593.
35. Kim EK, Choi E-J. Pathological roles of MAPK signaling pathways in human diseases. BBA Mol Basis Dis. 2010;1802:396–405. https://doi.org/10.1016/j.bbadis.2009.12.009.
36. Wehrend A, Meinecke B. Kinetics of meiotic progression, M-phase promoting factor (MPF) and mitogen-activated protein kinase (MAP kinase) activities during in vitro maturation of Porcine and bovine oocytes: species specific differences in the length of the meiotic stages. Anim Reprod Sci. 2001;66:175–84. https://doi.org/10.1016/s0378-4320(01)00094-x.
37. Han Y, Xia G, Tsang BK. Regulation of cyclin D2 expression and degradation by follicle-stimulating hormone during rat granulosa cell proliferation in vitro. Biol Reprod. 2013;88:57. https://doi.org/10.1095/biolreprod.112.105106.
38. Kawakami T, Kawakami Y, Kitaura J. Protein kinase C (PKC): nomal functions and dieases. J Biochem. 2002;132:677–82. https://doi.org/10.1093/oxfordjournals.jbchem.a003273.
39. Li Q, Park K, Li C, Rask-Madsen C, Mima A, Qi W, et al. Induction of vascular insulin resistance and endothelin-1 expression and acceleration of atherosclerosis by the overexpression of protein kinase C-β isoform in the endothelium. Circ Res. 2013;113:418–27. https://doi.org/10.1161/CIRCRESAHA.113.301074.
40. Martens H. Invited review: increasing milk yield and negative energy balance: a gordian knot for dairy cows? Animals-basel. 2023;13:3097. https://doi.org/10.3390/ani13193097.
41. Ringnér M. What is principal component analysis? Nat Biotechnol. 2008;26:303–4. https://doi.org/10.1038/nbt0308-303.
42. Jolliffe IT, Cadima J. Principal component analysis: a review and recent developments. Philos Trans R Soc Lond A Math Phys Eng Sci. 2016;374:20150202. https://doi.org/10.1098/rsta.2015.0202.
43. Lever J, Krzywinski M, Altman N. Principal component analysis. Nat Methods. 2017;14:641–2. https://doi.org/10.1038/nmeth.4346.
44. Conesa A, Madrigal P, Tarazona S, Gomez-Cabrero D, Cervera A, McPherson A, et al. A survey of best practices for RNA-seq data analysis. Genome Biol. 2016;17:13. https://doi.org/10.1186/s13059-016-0881-8.

Publisher's Note